European Journal of Radiology 190 (2025) 112234

Contents lists available at ScienceDirect

European Journal of Radiology

journal homepage: www.elsevier.com/locate/ejrad

Treatment response assessment in glioblastoma with GRASP DCE-MRI

Björn Vankan [b], Vichyat Var [b,c], Nikki Rommers [b,d], Marios N. Psychogios [b,c], Ramona A. Todea [a,b,c,*]

[a] Department of Neuroradiology, University Hospital Zurich, Rämistrasse 100, CH-8091 Zurich, Switzerland
[b] University of Basel, Petersplatz 1, 4001 Basel, Switzerland
[c] Department of Neuroradiology, Clinic of Radiology and Nuclear Medicine, University Hospital of Basel, Petersgraben 4, 4031 Basel, Switzerland
[d] Department of Clinical Research, University Hospital of Basel, Spitalstrasse 8/12, 4031 Basel, Switzerland

ARTICLE INFO

Keywords:
Treatment-related changes
Tumor progression
Glioblastoma
Signal-intensity time-curve analysis
GRASP DCE-MRI

ABSTRACT

Purpose: Following radiochemotherapy, glioblastoma patients often develop new or enlarging contrast-enhancing lesions, posing a critical challenge in distinguishing treatment-related changes (TRC) from tumor progression (TP). This study investigates the diagnostic accuracy of Golden Angle Radial Sparse Parallel Dynamic Contrast-Enhanced (GRASP DCE) MRI parameters derived from the signal intensity curve over time to discriminate TRC from TP.

Methods: Sixty-six glioblastoma patients, between 01/2017 and 12/2021, who underwent radiochemotherapy and developed new or enlarging contrast-enhancing lesions suspicious for TP, were analyzed. A diagnostic accuracy analysis using the area under the receiver operating characteristic curve (AUROC) assessed the effectiveness of GRASP DCE-MRI kinetic parameters in distinguishing TRC from TP.

Results: 138 DCE-MRI scans were classified into TRC (n = 63) vs. TP group (n = 75) according to the lesion outcome on serial MRI follow-up and the pathology results. The peak enhancement percentage (PE%), the initial area under the curve 30 s (iAUC 30) and 60 s (iAUC 60) were consistently lower in the TRC than in the TP group. Both PE% (Sensitivity 89 % (95 % CI [83, 96]), Specificity 87 % (95 % CI [78, 95])) and iAUC30 (Sensitivity 80 % [71, 88]), Specificity 81 % [71, 91]) showed very high accuracy in discriminating TRC from TP. The best threshold for PE% to differentiate both groups was 40.7 %.

Conclusion: Peak enhancement derived from GRASP DCE-MRI demonstrated the highest accuracy in distinguishing treatment-related changes from tumor progression in glioblastoma. This reproducible, easily interpretable metric may aid neuroradiologists in evaluating new or enlarging lesions post-radiochemotherapy, improving clinical decision-making.

1. Introduction

Glioblastoma is the most common malignant brain tumor in adults, with higher incidence in males (4.09/100000) [1]. The current standard treatment involves maximal safe resection followed by concurrent radiochemotherapy [2].

Assessing treatment response in glioblastoma relies on the updated RANO 2.0 (Response Assessment in Neuro-Oncology) criteria [3]. However, RANO 2.0 criteria struggles to differentiate TRC from TP particularly within the first 3 months after concurrent radiochemotherapy, due to the overlapping imaging patterns of TRC and TP [4–6]. Lesions with a higher tumor burden exhibit more neovascularization and leaky vasculature than those dominated by radionecrosis this characteristic that can be leveraged using DCE-MRI [6,7].

In DCE-MRI, contrast agent concentration is influenced by perfusion, capillary leakage, and interstitial volume. Early uptake primarily

Abbreviations: TP, Tumor progression; TRC, Treatment related changes; GTR, Gross total resection; GRASP DCE-MRI, Golden Angle Radial Sparse Parallel Dynamic Contrast-Enhanced MRI; RANO, Response assessment in neuro-oncology; RCT, Radiochemotherapy; iAUC, Initial area under the curve; iAUC30, The area under the initial 30 s of the signal intensity-time-curve; iAUC60, The area under the initial 60 s of the signal intensity-time-curve; KtransPE%, Peak Enhancement percentage; AUROC, Area under the receiver operating characteristic curve.

* Corresponding author at: Department of Neuroradiology, University Hospital Zurich, Rämistrasse 100, Zurich 8091, Switzerland.
E-mail addresses: bjoern.vankan@bluewin.ch (B. Vankan), vichyat.var@usb.ch (V. Var), Nikki.Rommers@usb.ch (N. Rommers), marios.psychogios@usb.ch (M.N. Psychogios), ramona.todea@usz.ch (R.A. Todea).

https://doi.org/10.1016/j.ejrad.2025.112234
Received 12 March 2025; Accepted 10 June 2025
Available online 13 June 2025

reflects perfusion and leakage, as backflux is minimal [8,9]. In malignant tumors, contrast reaches abnormal vessels and leaks into tissue faster than in benign ones, providing potential for distinguishing TP from TRC [10,8]. Semiquantitative parameters such as the peak enhancement percentage and the area under the signal intensity-time-curve can be directly derived from these curves, offering high reproducibility compared to complex pharmacokinetic modeling [8,9,11], and may aid in differentiating TRC from TP.

This study aims to assess the diagnostic accuracy of kinetic parameters extracted from GRASP DCE-MRI, including the peak enhancement percentage and the initial area under the curve in discriminating between treatment-related changes and tumor progression in glioblastoma patients.

2. Materials and methods

2.1. Study design

The study was approved by the ethics committee. All participants had written or waived informed consent. We performed a retrospective monocentric study, between 01/2017–12/2021, of patients with an integrative diagnosis of glioblastoma. The inclusion criteria were: (1) adult patients who underwent (2) surgery and postoperative RCT, (3) had contrast-enhanced (CE) postoperative MRI within 24 h, (4) developed new or enlarging contrast-enhancing lesions ≥10 × 10 mm, (5) had follow-up MRIs to assess the lesion outcome as TRC or TP and (6) had GRASP DCE-MRI. The exclusion criteria were: (1) missing consent, (2) incomplete MRI follow-up (Fig. 1).

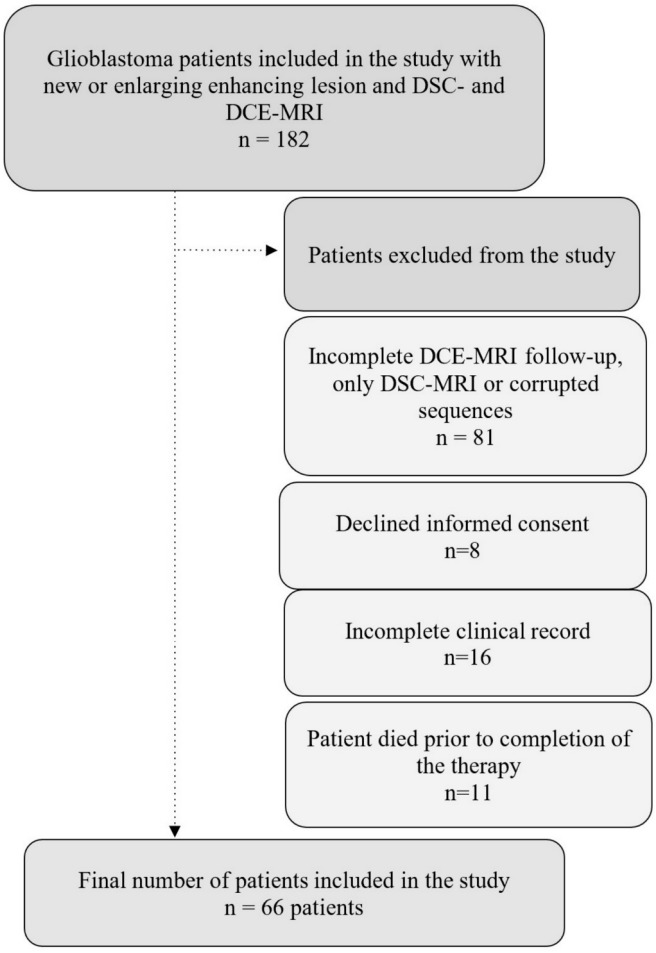

Fig. 1. Flow diagram with the patients included in the study.

This study builds on a cohort of 83 glioblastoma patients previously analyzed in an earlier study [12]. In this phase, the focus was put on evaluating the diagnostic accuracy of DCE-MRI in distinguishing treatment-related changes from tumor progression.

Study data were managed with the Research Electronic Data Capture (REDCap) software [13,14]

2.2. Imaging protocol

All MRI scans were performed with a 3T scanner (MAGNETOM Skyra, Siemens Healthineers) with a 20-channel head-neck coil. Contrast material: 20 ml Gadoteracid (0.5 mmol/ml, Dotarem® Guerbet), via 20G iv catheter. The treatment response was performed on T1-weighted post-contrast sequences according to the RANO 2.0 criteria. The dynamic sequences were acquired with a split-bolus technique where the first contrast bolus injected for the GRASP DCE-MRI served as preload to correct for T1-weighted leakage effects in a consecutive DSC−MRI acquisition [15,16]. To ensure that sufficient pre-contrast baseline data got recorded, the GRASP sequence was started 20 s prior to the contrast injection. The first 10 ml bolus of contrast was administered at an injection speed of 2.0 ml/s [17]. GRASP uses a continuous acquisition of k-space with the following parameters: TR 4.09 ms, TE 1.92 ms, flip angle 12°, FOV 240 mm, matrix size 256 × 256, voxel size 1.5-mm isotropic, radial views 850, slice partial Fourier 6/8, bandwidth 400 Hz/pixel, 4:23 min total acquisition. The dynamic images were reconstructed with a temporal resolution of 4.3 s [17].

2.3. Imaging analysis

One board-certified neuroradiologist Reader 1 (10 years of experience in radiology, 5 years in neuroradiology) assigned the 138 MRI follow-ups of the 66 patients to TRC (n = 63) or TP (n = 75) group according to the RANO criteria 2.0 and the lesion outcome on the follow-up MRI [18,6].

2.4. Definition of TRC and TP

TP was defined as a ≥25 % increase in sum of products of perpendicular diameters of enhancing lesions in comparison to baseline (first MRI performed after completion of RCT at 24–35 days) or to the nadir. Patients that had a new lesion outside of the radiotherapy field were directly considered TP [3]. To minimize the risk of misdiagnosing TRC as TP within the first three months post-RCT, available serial follow-up MRIs were taken into consideration until at least 3 months after the completion of RCT.

TRC was defined as stabilization, partial or complete resolution of a new lesion inside the irradiated volume without changes on therapy in the serial MRI follow-ups [3].

On pathology, lesions were classified as treatment-related changes/treatment response if characteristics such as “No mitosis”, “No vital tumor”, or “Necrosis with no vital tumor” were observed upon resection or biopsy. Lesions were classified as tumor if a percentage of mitosis between 5 % and, in very few cases, up to 20 % was present, or if there was evidence of “recurrence of the known glioblastoma”.

2.5. GRASP DCE-MRI analysis and postprocessing

The analysis of the signal intensity-time-curve of the DCE-MRI studies with the extraction of the PE% and the iAUC 30 and iAUC 60 as parameters was performed using the postprocessing tool Olea Sphere v3.0 (Olea Medical SAS, La Ciotat, France) by Reader 1 and Reader 2 (Radiology resident “in training”), both blinded to the lesion outcome at the time of the measurements. For each lesion at least two regions of interest (of at least 10 × 10 mm) were defined at the level of the “hotspot” in the color-coded maps.

The value of the maximum PE% was automatically provided by the

Olea software. The iAUC30 and iAUC60 were calculated using the trapezoidal method by two other readers Reader 3 and Reader 4.

2.6. Statistical analysis

The comparison of perfusion parameters between groups was performed using the Wilcoxon rank sum test. The best threshold for the respective parameter for discriminating between TRC and TP was determined by maximizing Youden's index at a minimum sensitivity of 60%. Diagnostic accuracy was based on the respective best threshold value that results in the best combination of specificity and sensitivity for discrimination of the two TRC groups. The TP are considered as "cases" (i.e. true positive), and the TRC as "controls" (i.e. true negative).

The Receiver operating characteristic curve curve with its 95 % confidence interval (CI) (according to DeLong's method to define the variance of the AUC) was used to evaluate the accuracy of the perfusion parameters to discriminate TRC from TP [19]. Furthermore, sensitivity and specificity were calculated with bootstrap resampling and averaging methods by Fawcett [20]. The accuracy for the best cut-off was calculated with 95 % CI according to Blaker [21]. All statistical analyses were performed in R [22].

A diagnostic accuracy analysis of PE%, iAUC30, and iAUC60 was first conducted to identify a threshold that could discriminate between TRC and TP following the completion of radiochemotherapy. Given the challenges of the RANO 2.0 criteria in differentiating TRC from TP, particularly within the first 3 months post-radiochemotherapy, a second analysis was conducted using only MRIs from the first 3 months to establish thresholds and assess diagnostic accuracy, aiming to offer a preliminary distinction between TP and TRC.

"This article follows the STARD reporting guidelines."

3. Results

3.1. Baseline characteristics of the patients

The final cohort encompassed 66 patients (the mean age was 59 ± 13 years, 42 males). All patients underwent surgery for both diagnostic and treatment purposes. Of these, 51 received combined radiochemotherapy with Temozolomide, 45 received additional Temozolomide, and 15 were treated with radiotherapy alone as part of first-line therapy. 9 patients had a re-resection (See Table 1 and Fig. 1).

In total 138 scans were analyzed and classified into the TRC (n = 63 MRI scans) and TP (n = 75 MRI scans) group according to the MRI follow-up. 9 follow-ups were also confirmed histological and molecular as being a tumor progression.

Table 1
Baseline characteristics of the patients.

Characteristic	Total (n = 66)
Mean age (SD)	59 (13)
Gender – M/F (%)	42 (64,6 %), 23 (35.4 %)
Glioblastoma integrated diagnosis	66
Operation Type	
Complete resection	24
Subtotal resection	34
Biopsy	8
Re-resection	9/66 patients
Combined radiochemotherapy with Temozolomide	51
Radiotherapy alone	15
Additive phase with Temozolomide	45
Number of MRI visits analysed according to RANO 2.0 and the correspondent DCE-MRI perfusion studies	
Total	138
Classified as TRC	63
Classified as TP	75
Histologic confirmation after re-resection	9 (TP cases)

Multiple visits per patient were available with a mean number of scans per patient of 2.62 (SD: 1.08). All MRI follow-ups were considered independent of one another. Therefore, it was concluded that no corrections were needed to account for multiple scans in one patient. Within the first 3 months after completing RCT, 33 MRI follow-ups were classified as TRC and 29 as TP. Therefore, for the diagnostic accuracy analysis of DCE-MRI in discriminating between TRC and TP during this period, 62 DCE-MRI perfusion studies were analyzed.

3.2. Diagnostic accuracy of GRASP DCE-MRI to discriminate TRC from TP in different time windows after completion of RCT

The PE% was consistently lower in the TRC group than in the TP group. The median PE% with [Interquartile range (IQR)] for TRC vs. TP was 29 % [26, 35] vs. 53 % [45, 69]. The best threshold to discriminate between both groups was 40.7 % (AUC: 0.94, sensitivity: 89 %, specificity: 87 %, accuracy: 88 %) (See Table 2 and Fig. 2).

The median iAUC30 was also consistently lower in the TRC group than in the TP group. The iAUC30 for TRC vs. TP with [IQR] was 949 [756, 1196] vs. 1633 [1340, 2058]. The best threshold was 1304, (AUC: 0.90, sensitivity: 80 %, specificity: 81 %, accuracy: 80 %).

The iAUC60 was also consistently lower in the TRC group than in the TP group: The median iAUC60 with [IQR] for TRC was 1847 [1439, 2386] vs. 3337 [2670, 3965] for TP. The best threshold was 2614 (AUC: 0.89, sensitivity: 79 %, specificity: 83 %, accuracy: 80 %) (See Table 2**).**

The second analysis considering the diagnostic accuracy of PE%, iAUC30 and iAUC60 within the first 3 months after completion of radiochemotherapy also consistently showed a high diagnostic accuracy and similar values of the permeability parameters compared to the first analysis. For instance, the median PE% within the first 3 months post-RCT was 29 % [26, 34] for TRC and 62 % [49, 69] for TP, with an optimal threshold of 49 % (AUC 0.93, sensitivity: 76 %, specificity: 100 %, accuracy: 89 %) (See Table 2 and Fig. 2**).**

4. Discussion

Assessing treatment response in glioblastoma patients after radiochemotherapy remains challenging particularly within the first 3 months, due to overlapping imaging patterns between treatment-related changes and persistent or progressive tumor on morphologic sequences [3–6]. Accurate differentiation between these two phenomena is crucial to prevent unnecessary treatment escalation and exposure of patients to less effective second-line therapies [6].

This study evaluates the diagnostic accuracy of the peak-enhancement percentage and the initial area under the curve at 30 s and 60 s, derived from the GRASP DCE-MRI signal intensity-time curve, in discriminating between TRC and TP after radiochemotherapy in glioblastoma patients. Additionally, it aims to identify threshold values for these metrics that could discriminateTRC from TP.

Analysis of 138 MRI follow-ups (01/2017–12/2021) in 66 glioblastoma patients found that the PE% had the highest diagnostic accuracy among the tested parameters, achieving 88 % accuracy (sensitivity 89 %; specificity of 87 %, AUC 0.94) in discriminating TRC from TP. PE was consistently lower in the TRC group (29 % [IQR: 26, 35]) than in the TP group (53 % [IQR: 45, 69]) with an optimal threshold to discriminate between both groups of 40.7 % (see Table 2, Fig. 2). The iAUC30 and the iAUC60 showed similar performance, slightly lower than the PE%, but maintained high diagnostic accuracy at 80 % for both parameters (See Table 2).

The second analysis assessed the diagnostic value of semi-quantitative DCE-MRI parameters to discriminate between TRC and TP within the first 3 months after RCT, a period when RANO criteria are less effective [18]. Results showed that DCE-MRI parameters maintained high diagnostic accuracy with similar threshold values in this early phase. For instance, PE% within the first 3 months post-RCT was 29 % [IQR: 26, 34] for TRC and 62 % [49, 69] for TP, with an optimal

Table 2
Diagnostic accuracy of the DCE-MRI parameters (PE%, iAUC 30 and iAUC 60) in discriminating between TRC and TP in glioblastoma patients after the completion of post-surgical radiochemotherapy. The absolute values of the PE%, iAUC30 and iAUC60 in the TRC and TP group are expressed as median [25th percentile, 75th percentile]. Accuracy, sensitivity, specificity and AUC are presented with 95% confidence interval.

DCE-MRI parameter	TRC group	TP group	Threshold	Accuracy	Sensitivity	Specificity	AUC
PE% value							
Independent of the period after RCT	29 [26, 35]	53 [45, 69]	40.7	88 [82,93]	89 [83, 96]	87 [78, 95]	0.94 [0.89, 0.98]
Within 3 months post-RCT	29 [26,34]	62 [49,69]	48.9	89 [79,95]	76 [59,90]	100 [100, 100]	0.93 [0.86 1]
iAUC30							
Independent of the period after RCT	949 [756, 1196]	1633 [1340, 2058]	1304	80[73,86]	80 [71, 88]	81 [71, 91]	0.90 [0.85, 0.95]
Within 3 months after RCT	911 [703,1196]	1685 [1419,2076]	1116	84 [73,92]	97 [90,100]	73 [58,88]	0.92 [0.85,0.98]
iAUC60							
Independent of the period after RCT	1847 [1439, 2386]	3337 [2670, 3965]	2614	80 [73,86]	79 [69, 87]	83 [73, 92]	0.89 [0.84, 0.94]
Within 3 months after RCT	1847 [1310,2271]	3383 [3063,4071]	3050	86 [75,92]	76 [59,90]	94 [85, 100]	0.91 [0.84, 0.98]

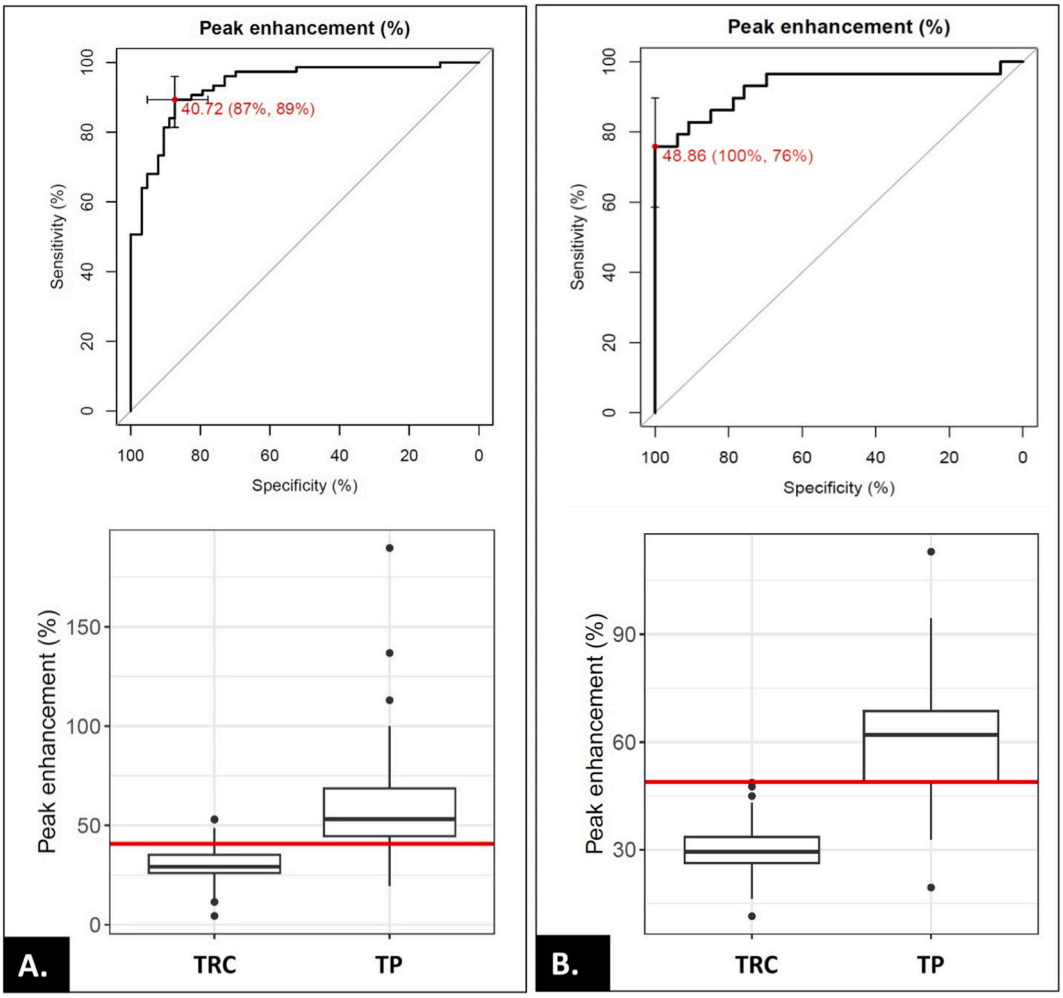

Fig. 2. Diagnostic accuracy of the PE% and the best threshold with corresponding specificity and sensitivity to discriminate TRC from TP independent of the time-window after RCT in **A.** and within 3 months after completion of radiochemotherapy in **B.**

threshold of 49 % (sensitivity: 76 %, specificity: 100 %, accuracy: 89 %) (see Table 2 and Fig. 2).

These results suggest that when facing with a new or enlarging contrast-enhancing lesion suspicious of progressive disease in a patient with glioblastoma after radiochemotherapy, even within the first 3 months post-RCT, a PE% threshold of 40.7 % could help distinguish TRC from TP. The iAUC30 and iAUC60 also showed higher values in TP than in TRC. Ultimately, when visually assessing the signal intensity-time-curve derived from DCE-MRI a slow or mild initial rise (PE% $\leq$ 40.7 %) with a plateau phase suggests TRC, while a rapid rise (PE% $>$ 49 %) followed by a plateau or washout phase indicates TP (see Figs. 3 and 4).

DSC-MRI remains the most widely used perfusion technique, particularly through rCBV (relative cerebral blood volume), which helps differentiate glioma grades and distinguish TRC from TP [23–25]. While DCE-MRI has shown valuable results in neurooncology, its adoption has been limited by variability in protocols and complex post-processing

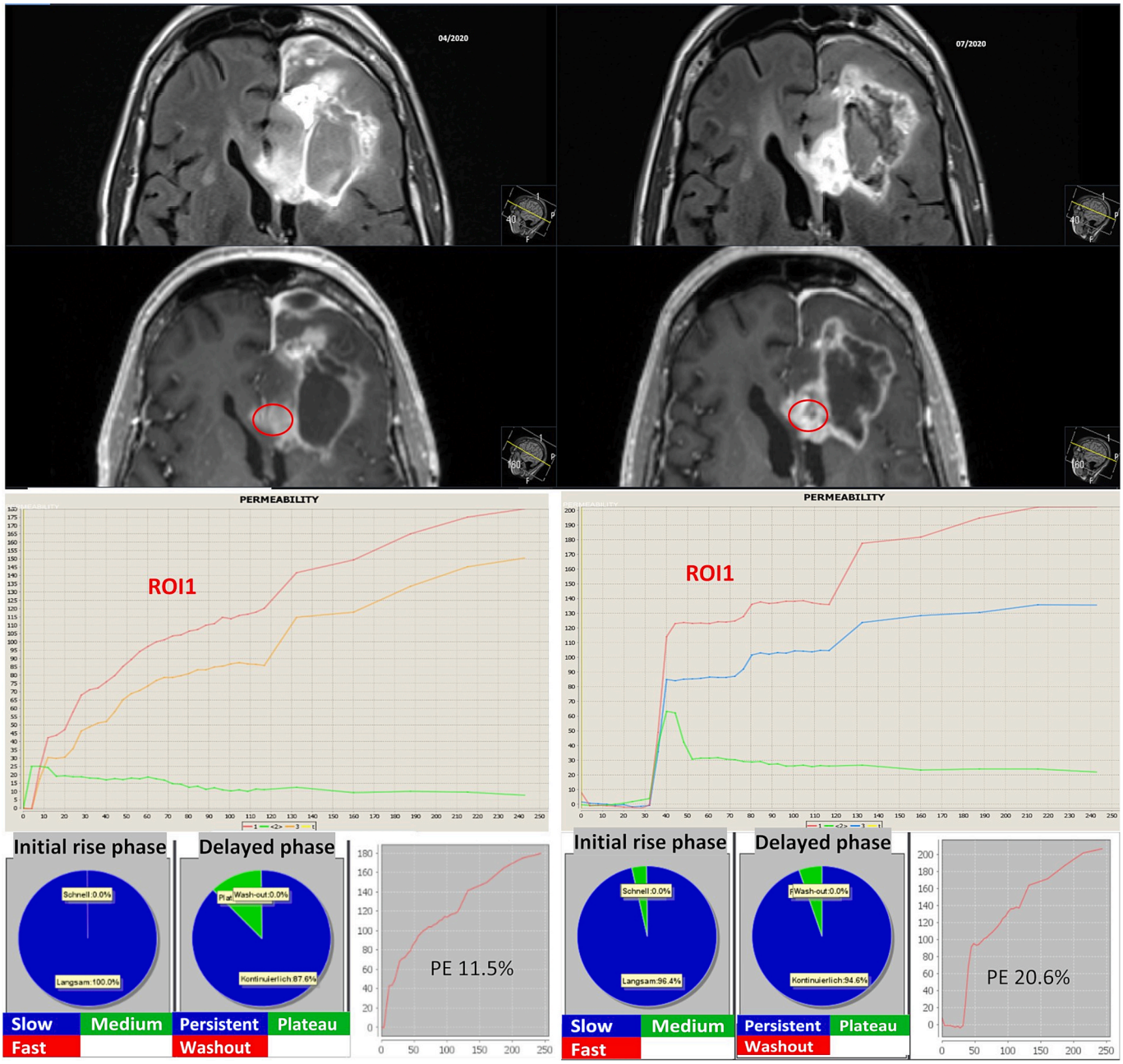

Fig. 3. 50-year-old patient initially classified with tumor progression at 1 month and stable disease at 3 months after radiochemotherapy, according to the RANO 2.0 criteria. DCE-MRI kinetic analysis indicated treatment-related changes at both 1- and 3-months post-RCT. The top row displays transversal FLAIR and contrast-enhanced T1 MPRAGE images, showing a new contrast-enhancing lesion in the radiotherapy field around the resection cavity, which remained stable between the two follow-ups. The signal-intensity-curve from the initial examination showed a peak enhancement of 11.5 %, and 20.6 % at the subsequent follow-up, both suggesting a response to first-line treatment.

[7,24,26–32].

To address these challenges, this study underscores the value of semiquantitative analysis, offering reproducible metrics without the need for pharmacokinetic modeling, and builds on prior research demonstrating high diagnostic accuracy of DCE-MRI-derived parameters like iAUC and AUCR for distinguishing early tumor progression from pseudoprogression. In a study of 51 glioblastoma patients (15 with TRC and 36 with TP), who underwent DCE scans every three months starting within 2 months after radiochemotherapy, H. Jing et al. reported a similar high diagnostic accuracy for the DCE-MRI derived iAUC (sensitivity: 88.9 %, specificity: 100 %) [30]. Suh et al. [31] studied 99 patients with new or enlarged lesions on follow-up MRI who underwent DCE scans 4–5 weeks after radiochemotherapy. They found that DCE-MRI parameters, including mAUCRH, AUCR50, AUCR75, AUCR90, and AUCRMODE, can differentiate early tumor progression from pseudoprogression. Consistent with the findings of this study, their study showed that AUCR50, representing blood flow and volume, had the highest specificity (87.2 % sensitivity, 83.1 % specificity), while mAUCRH showed the highest sensitivity (90.1 % sensitivity, 82.9 % specificity).

In our standard tumor protocol we have integrated both DCE- and DSC-MRI with the split bolus technique [16,12] with an improved DCE-MRI technique, the GRASP (Golden-angle radial sparse parallel) method [33,34], which provides both high spatial and temporal resolution that allows a reliable analysis of the permeability parameters.

This study's limitations are related to its retrospective design which

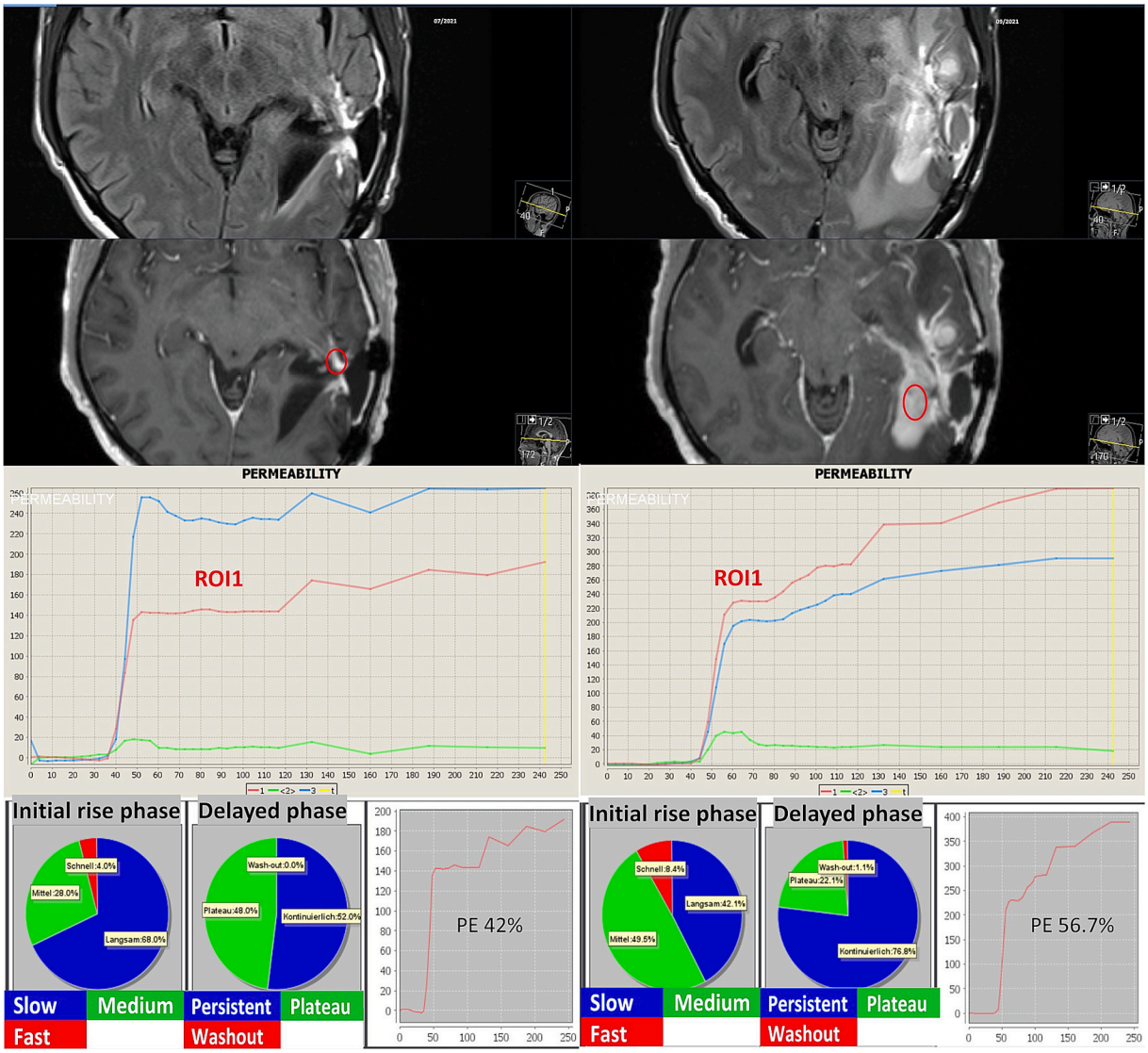

Fig. 4. 46-year-old patient with tumor progression according to the RANO 2.0 criteria and in the DCE-MRI analysis. The top row displays transversal FLAIR and contrast-enhanced T1 MPRAGE images, showing a new contrast-enhancing lesion in the radiotherapy field around the resection cavity that progressed between the first MRI at 12 weeks and the subsequent follow-up at 20 weeks post-radiochemotherapy. The signal intensity curve analysis for the initial scan showed a peak enhancement of 42 %, which increased to 56.7 % at the follow-up, both indicating tumor progression.

introduces selection bias. Additionally, while PE% is automatically generated, manually selecting start points for iAUC30 and iAUC60 may have introduced variability. Larger confidence intervals within the first three months post-RCT likely reflect the smaller sample size.

5. Conclusions

Semiquantitative analysis of GRASP DCE-MRI parameters demonstrated high diagnostic accuracy in distinguishing TRC from TP in glioblastoma patients after radiochemotherapy. These easy-to interpret parameters could enhance neuroradiologists' diagnostic confidence, improve treatment response evaluation, and complement RANO-based assessments in routine clinical practice.

Data sharing

Data generated or analyzed during the study are available from the corresponding author by request.

CRediT authorship contribution statement

Björn Vankan: Conceptualization, Formal analysis, Investigation, Methodology, Validation, Visualization, Writing – original draft, Writing – review & editing. **Vichyat Var:** Conceptualization, Formal analysis, Investigation, Methodology, Visualization, Writing – original draft, Writing – review & editing. **Nikki Rommers:** Formal analysis, Investigation, Methodology, Resources, Validation, Writing – original draft, Writing – review & editing. **Marios N. Psychogios:** Conceptualization, Investigation, Resources, Software, Supervision, Writing – review & editing. **Ramona A. Todea:** Conceptualization, Data curation, Formal analysis, Funding acquisition, Investigation, Methodology, Project administration, Supervision, Validation, Visualization, Writing – original draft, Writing – review & editing.

Funding

The study was supported by an institutional grant offered in 2022 by the University of Basel Research Fund for Excellent Junior Researchers: Nr. 3MS1090. The corresponding author has benefitted of the grant.

Declaration of competing interest

The authors declare the following financial interests/personal relationships which may be considered as potential competing interests: Ramona-Alexandra Todea reports a relationship with University of Basel that includes: funding grants. The other authors, they declare that they have no known competing financial interests or personal relationships that could have appeared to influence the work reported in this paper.

References

[1] Q.T. Ostrom, M. Price, C. Neff, G. Cioffi, K.A. Waite, C. Kruchko, J.S. Barnholtz-Sloan, CBTRUS Statistical Report: Primary Brain and Other Central Nervous System Tumors Diagnosed in the United States in 2016-2020, Neuro Oncol. 25(12 Suppl 2) (2023) iv1–iv99. doi: 10.1093/neuonc/noad149.

[2] R. Stupp, W.P. Mason, M.J. van den Bent, M. Weller, B. Fisher, M.J. Taphoorn, K. Belanger, A.A. Brandes, C. Marosi, U. Bogdahn, J. Curschmann, R.C. Janzer, S. K. Ludwin, T. Gorlia, A. Allgeier, D. Lacombe, J.G. Cairncross, E. Eisenhauer, R. O. Mirimanoff, Radiotherapy plus concomitant and adjuvant temozolomide for glioblastoma, N. Engl. J. Med. 352 (10) (2005) 987–996, https://doi.org/10.1056/NEJMoa043330.

[3] P.Y. Wen, M. van den Bent, G. Youssef, T.F. Cloughesy, B.M. Ellingson, M. Weller, E. Galanis, D.P. Barboriak, J. de Groot, M.R. Gilbert, R. Huang, A.B. Lassman, M. Mehta, A.M. Molinaro, M. Preusser, R. Rahman, L.K. Shankar, R. Stupp, J.E. Villanueva-Meyer, W. Wick, D.R. Macdonald, D.A. Reardon, M.A. Vogelbaum, S.M. Chang, RANO 2.0: Update to the Response Assessment in Neuro-Oncology Criteria for High- and Low-Grade Gliomas in Adults, J. Clin. Oncol. 41(33) (2023) 5187–5199. doi: 10.1200/jco.23.01059.

[4] C. Le Fèvre, J.M. Constans, I. Chambrelant, D. Antoni, C. Bund, B. Leroy-Freschini, R. Schott, H. Cebula, G. Noël, Pseudoprogression versus true progression in glioblastoma patients: a multiapproach literature review. Part 2 - Radiological features and metric markers, Crit. Rev. Oncol. Hematol. 159 (2021) 103230, https://doi.org/10.1016/j.critrevonc.2021.103230.

[5] C. Le Fèvre, B. Lhermitte, G. Ahle, I. Chambrelant, H. Cebula, D. Antoni, A. Keller, R. Schott, A. Thiery, J.M. Constans, G. Noël, Pseudoprogression versus true progression in glioblastoma patients: a multiapproach literature review: Part 1 - Molecular, morphological and clinical features, Crit. Rev.Oncol. Hematol. 157 (2021) 103188, https://doi.org/10.1016/j.critrevonc.2020.103188.

[6] P.Y. Wen, M. Weller, E.Q. Lee, B.M. Alexander, J.S. Barnholtz-Sloan, F.P. Barthel, T.T. Batchelor, R.S. Bindra, S.M. Chang, E.A. Chiocca, T.F. Cloughesy, J.F. DeGroot, E. Galanis, M.R. Gilbert, M.E. Hegi, C. Horbinski, R.Y. Huang, A.B. Lassman, E. Le Rhun, M. Lim, M.P. Mehta, I.K. Mellinghoff, G. Minniti, D. Nathanson, M. Platten, M. Preusser, P. Roth, M. Sanson, D. Schiff, S.C. Short, M.J.B. Taphoorn, J.C. Tonn, J. Tsang, R.G.W. Verhaak, A. von Deimling, W. Wick, G. Zadeh, D.A. Reardon, K. D. Aldape, M.J. van den Bent, Glioblastoma in adults: a Society for Neuro-Oncology (SNO) and European Society of Neuro-Oncology (EANO) consensus review on current management and future directions, Neuro Oncol. 22 (8) (2020) 1073–1113, https://doi.org/10.1093/neuonc/noaa106.

[7] J. Wu, Z. Liang, X. Deng, Y. Xi, X. Feng, Z. Yao, Z. Shu, Q. Xie, Glioma grade discrimination with dynamic contrast-enhanced MRI: an accurate analysis based on MRI guided stereotactic biopsy, Magn. Reson. Imaging 99 (2023) 91–97, https://doi.org/10.1016/j.mri.2023.02.003.

[8] X. Li, W. Huang, J.H. Holmes, Dynamic contrast-enhanced (DCE) MRI, Magn. Reson. Imaging Clin. N. Am. 32 (1) (2024) 47–61, https://doi.org/10.1016/j.mric.2023.09.001.

[9] C.A. Cuenod, D. Balvay, Perfusion and vascular permeability: basic concepts and measurement in DCE-CT and DCE-MRI, Diagn. Interv. Imaging 94 (12) (2013) 1187–1204, https://doi.org/10.1016/j.diii.2013.10.010.

[10] J. Wu, et al., Glioma grade discrimination with dynamic contrast-enhanced MRI: Anaccurate analysis based on MRI guided stereotactic biopsy, MagneUc Resonance Imaging 99 (2023) 91–97.

[11] P.S. Tofts, G. Brix, D.L. Buckley, J.L. Evelhoch, E. Henderson, M.V. Knopp, H. B. Larsson, T.Y. Lee, N.A. Mayr, G.J. Parker, R.E. Port, J. Taylor, R.M. Weisskoff, Estimating kinetic parameters from dynamic contrast-enhanced T(1)-weighted MRI of a diffusable tracer: standardized quantities and symbols, J. Magn. Reson. Imaging 10 (3) (1999) 223–232, https://doi.org/10.1002/(sici)1522-2586(199909)10:3<223::aid-jmri2>3.0.co;2-s.

[12] Vichyat Var, Severina M. Leu, Nikki Rommers, Marios N. Psychogios, Dominik Cordier, Ramona A. Todea, Differentiation of tumor progression from pseudoprogression in glioblastoma patients with GRASP DCE-MRI and DSC-MRI, Journal of Neuroradiology, Volume 52, Issue 4, 2025, 101354, ISSN 0150-9861.

[13] P.A. Harris, et al., Research electronic data capture (REDCap)–a metadata-driven methodology and workflow process for providing translational research informatics support, J Biomed Inform 42 (2) (2009) 377–381, https://doi.org/10.1016/j.jbi.2008.08.010.

[14] P.A. Harris, et al., The REDCap consortium: Building an international community of software platform partners, J Biomed Inform 95 (2019) 103208, https://doi.org/10.1016/j.jbi.2019.103208.

[15] M. Essig, et al., MR imaging of neoplastic central nervous system lesions: review andrecommendations for current practice, AJNR Am J Neuroradiol 33 (5) (2012) 803–817.

[16] M. Essig, T.B. Nguyen, M.S. Shiroishi, M. Saake, J.M. Provenzale, D.S. Enterline, N. Anzalone, A. Dörfler, À. Rovira, M. Wintermark, M. Law, Perfusion MRI: the five most frequently asked clinical questions, AJR Am. J. Roentgenol. 201 (3) (2013) W495–W510, https://doi.org/10.2214/ajr.12.9544.

[17] L. Feng, Golden-angle radial MRI: basics, advances, and applications, J. Magn. Reson. Imaging 56 (1) (2022) 45–62, https://doi.org/10.1002/jmri.28187.

[18] P.Y. Wen, et al., *RANO 2.0: Update to the Response Assessment in Neuro-Oncology Criteria for High- and Low-Grade Gliomas in Adults*, J Clin Oncol 41 (33) (2023) 5187–5199.

[19] E.R. DeLong, D.M. DeLong, D.L. Clarke-Pearson, Comparing the areas under two or more correlated receiver operating characteristic curves: a nonparametric approach, Biometrics 44 (3) (1988) 837–845.

[20] T. Fawcett, An introduction to ROC analysis, Pattern Recogn. Lett. 27 (8) (2006) 861–874, https://doi.org/10.1016/j.patrec.2005.10.010.

[21] H. Blaker, Confidence curves and improved exact confidence intervals for discrete distributions, Can. J. Statist./La Revue Canadienne De Statistique 28 (4) (2000) 783–798, https://doi.org/10.2307/3315916.

[22] X. Robin, N. Turck, A. Hainard, N. Tiberti, F. Lisacek, J.C. Sanchez, M. Müller, pROC: an open-source package for R and S+ to analyze and compare ROC curves, BMC Bioinf. 12 (2011) 77, https://doi.org/10.1186/1471-2105-12-77.

[23] R. Bammer, S.A. Amukotuwa, Dynamic susceptibility contrast perfusion, Part 1: the Fundamentals, Magn. Reson. Imaging Clin. N. Am. 32 (1) (2024) 1–23, https://doi.org/10.1016/j.mric.2023.09.010.

[24] O.M. Henriksen, M. del Mar Álvarez-Torres, P. Figueiredo, G. Hangel, V.C. Keil, R. E. Nechifor, F. Riemer, K.M. Schmainda, E.A.H. Warnert, E.C. Wiegers, T.C. Booth, High-grade glioma treatment response monitoring biomarkers: a position statement on the evidence supporting the use of advanced MRI techniques in the clinic, and the latest bench-to-bedside developments. part 1: perfusion and diffusion techniques, Front. Oncol. 12 (2022), https://doi.org/10.3389/fonc.2022.810263.

[25] A. Anil, A.M. Stokes, R. Chao, L.S. Hu, L. Alhilali, J.P. Karis, L.C. Bell, C.C. Quarles, Identification of single-dose, dual-echo based CBV threshold for fractional tumor burden mapping in recurrent glioblastoma, Front. Oncol. 13 (2023) 1046629, https://doi.org/10.3389/fonc.2023.1046629.

[26] A. Berger, M.D. Lee, E. Lotan, K.T. Block, G. Fatterpekar, D. Kondziolka, Distinguishing brain metastasis progression from radiation effects after stereotactic radiosurgery using longitudinal GRASP dynamic contrast-enhanced MRI, Neurosurgery 92 (3) (2023) 497–506, https://doi.org/10.1227/neu.0000000000002228.

[27] K.E. Shin, K.J. Ahn, H.S. Choi, S.L. Jung, B.S. Kim, S.S. Jeon, Y.G. Hong, DCE and DSC MR perfusion imaging in the differentiation of recurrent tumour from treatment-related changes in patients with glioma, Clin. Radiol. 69 (6) (2014) e264–e272, https://doi.org/10.1016/j.crad.2014.01.016.

[28] K. Nael, A.H. Bauer, A. Hormigo, M. Lemole, I.M. Germano, J. Puig, B. Stea, Multiparametric MRI for differentiation of radiation necrosis from recurrent tumor in patients with treated glioblastoma, AJR Am. J. Roentgenol. 210 (1) (2018) 18–23, https://doi.org/10.2214/ajr.17.18003.

[29] J. Arevalo-Perez, A. Trang, E. Yllera-Contreras, O. Yildirim, A. Saha, R. Young, J. Lyo, K.K. Peck, A.I. Holodny, Longitudinal evaluation of DCE-MRI as an early indicator of progression after standard therapy in glioblastoma, Cancers 16 (10) (2024) 1839.

[30] H. Jing, X. Yan, J. Li, D. Qin, N. Zhang, H. Zhang, The value of dynamic contrast-enhanced magnetic resonance imaging (DCE-MRI) in the differentiation of pseudoprogression and recurrence of intracranial gliomas, Contrast Media Mol. Imaging 2022 (2022) 5680522, https://doi.org/10.1155/2022/5680522.

[31] C.H. Suh, H.S. Kim, Y.J. Choi, N. Kim, S.J. Kim, Prediction of pseudoprogression in patients with glioblastomas using the initial and final area under the curves ratio derived from dynamic contrast-enhanced T1-weighted perfusion MR imaging, AJNR Am. J. Neuroradiol. 34 (12) (2013) 2278–2286, https://doi.org/10.3174/ajnr.A3634.

[32] A.A. Thomas, J. Arevalo-Perez, T. Kaley, J. Lyo, K.K. Peck, W. Shi, Z. Zhang, R. J. Young, Dynamic contrast enhanced T1 MRI perfusion differentiates pseudoprogression from recurrent glioblastoma, J. Neurooncol 125 (1) (2015) 183–190, https://doi.org/10.1007/s11060-015-1893-z.

[33] L. Heacock, Y. Gao, S.L. Heller, A.N. Melsaether, J.S. Babb, T.K. Block, R. Otazo, S. G. Kim, L. Moy, Comparison of conventional DCE-MRI and a novel golden-angle radial multicoil compressed sensing method for the evaluation of breast lesion conspicuity, J. Magn. Reson. Imaging 45 (6) (2017) 1746–1752, https://doi.org/10.1002/jmri.25530.

[34] L. Feng, R. Grimm, K.T. Block, H. Chandarana, S. Kim, J. Xu, L. Axel, D. K. Sodickson, R. Otazo, Golden-angle radial sparse parallel MRI: combination of compressed sensing, parallel imaging, and golden-angle radial sampling for fast and flexible dynamic volumetric MRI, Magn. Reson. Med. 72 (3) (2014) 707–717, https://doi.org/10.1002/mrm.24980.